ADVANCED MATERIALS

Supporting Information

for *Adv. Mater.*, DOI 10.1002/adma.202211244

Self-Organization of Iron Sulfide Nanoparticles into Complex Multicompartment Supraparticles

E. Sumeyra Turali-Emre, Ahmet E. Emre, Drew A. Vecchio, Usha Kadiyala, J. Scott VanEpps and Nicholas A. Kotov**

Supporting Information

Self-Organization of Iron Sulfide Nanoparticles into Multicompartment Supraparticles

E. Sumeyra Turali-Emre, Ahmet E. Emre, Drew Vecchio, Usha Kadiyala, J. Scott VanEpps, and Nicholas A. Kotov**

Contains:

1. 14 Nanocup assembly

REFERENCES

Figure S1-S21

Table S1-S5

1.1 Self-Assembled Structures on the pathway from NPs to mSPs

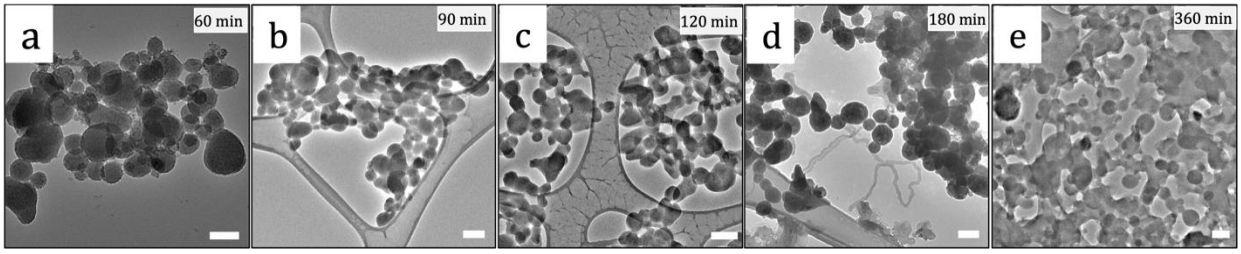

Figure S1 TEM images of NPs and synthesis reaction time points at (a) 60, (b) 90, (c) 120, (d) 180 and (e) 360min. Scale bars: 100nm

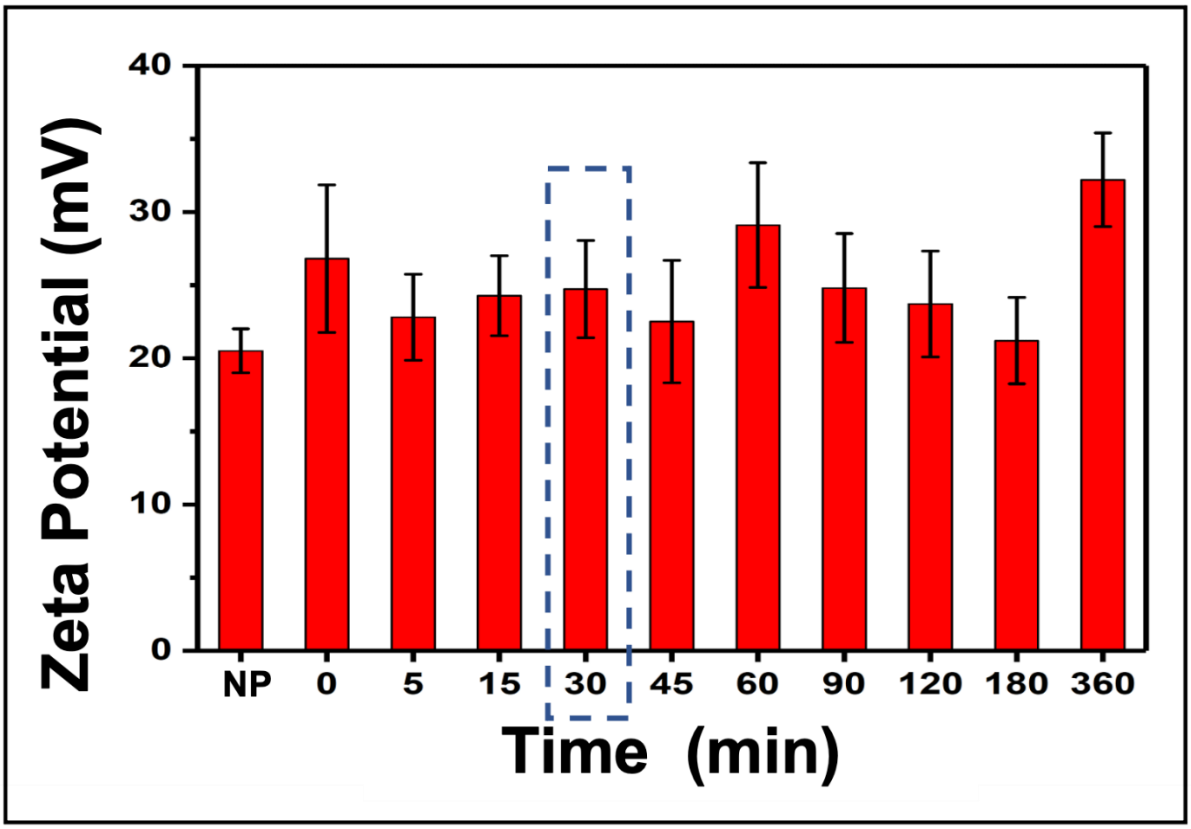

Figure S2 Zeta potential of synthesis reaction time points at NP, 0, 5, 15, 30, 60, 90, 120, 180 and 360min.

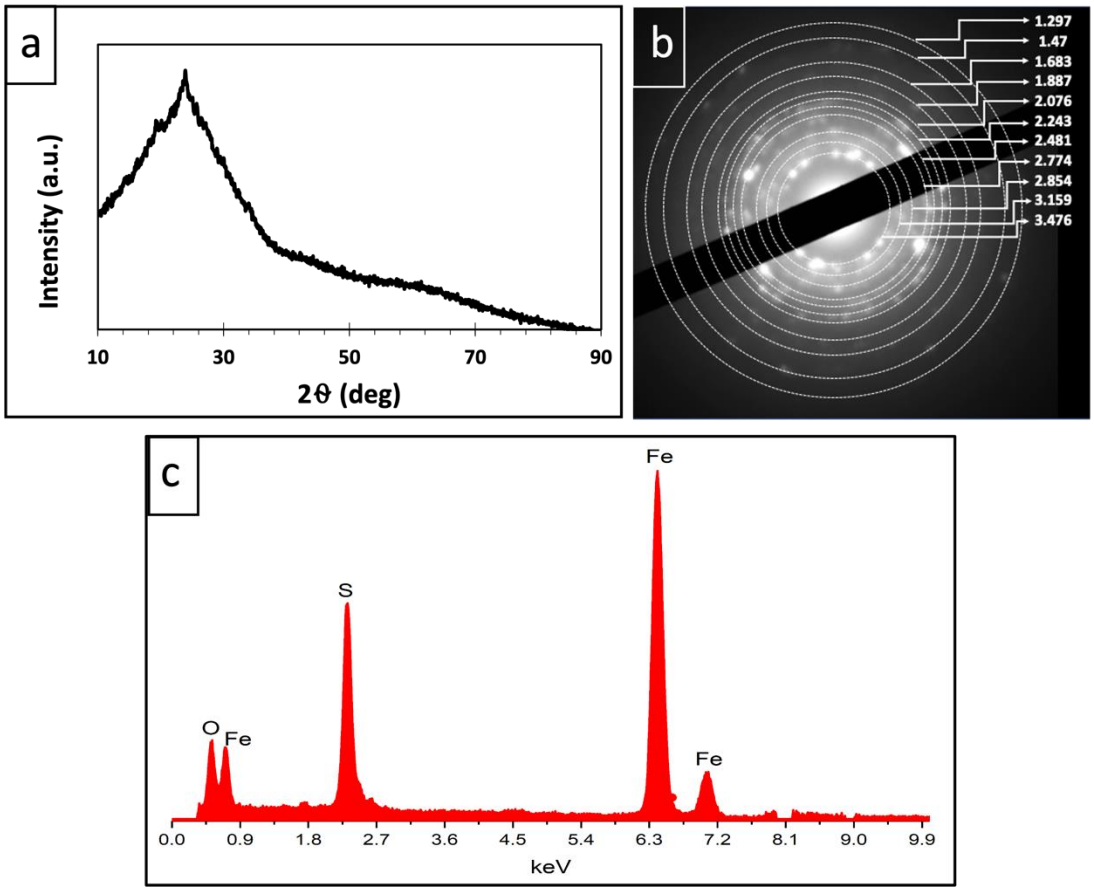

Figure S3 (a) XRD data of constituent NPs. (b) SAED of constituent NPs and corresponding d-spacing of each diffraction ring. (c) EDS analysis data of constituent NPs, background subtracted.

Table S1 Comparison of d-spacing of NPs *vs*. FeS_2 and Fe_2O_3

NP	**FeS_2 (Pnnm)**		**FeS_2 (Pa-3)**		**Fe_2O_3 (Aba2)**	
d-spacing	d(hkl)	hkl	d(hkl)	hkl	d(hkl)	hkl
3.476	3.4313	110				
3.159			3.1339	111	3.262	200
2.854	2.8677	011			2.9371	111
2.774	2.689	101	2.7141	200		
2.481	2.4083	111	2.4275	210	2.351	020
2.243	2.218	200	2.216	211	2.2118	120
2.076	2.0524	210	1.9191	220	1.9073	220
1.887	1.7545	211	1.8094	221	1.8805	202
1.683	1.5921	031	1.6366	311	1.6446	022
1.47	1.3998	230	1.4507	321	1.4685	222
1.297	1.2977	320	1.2794	411	1.2256	331

*Components of this table is chosen based on selected area electron diffraction (SAED) analysis

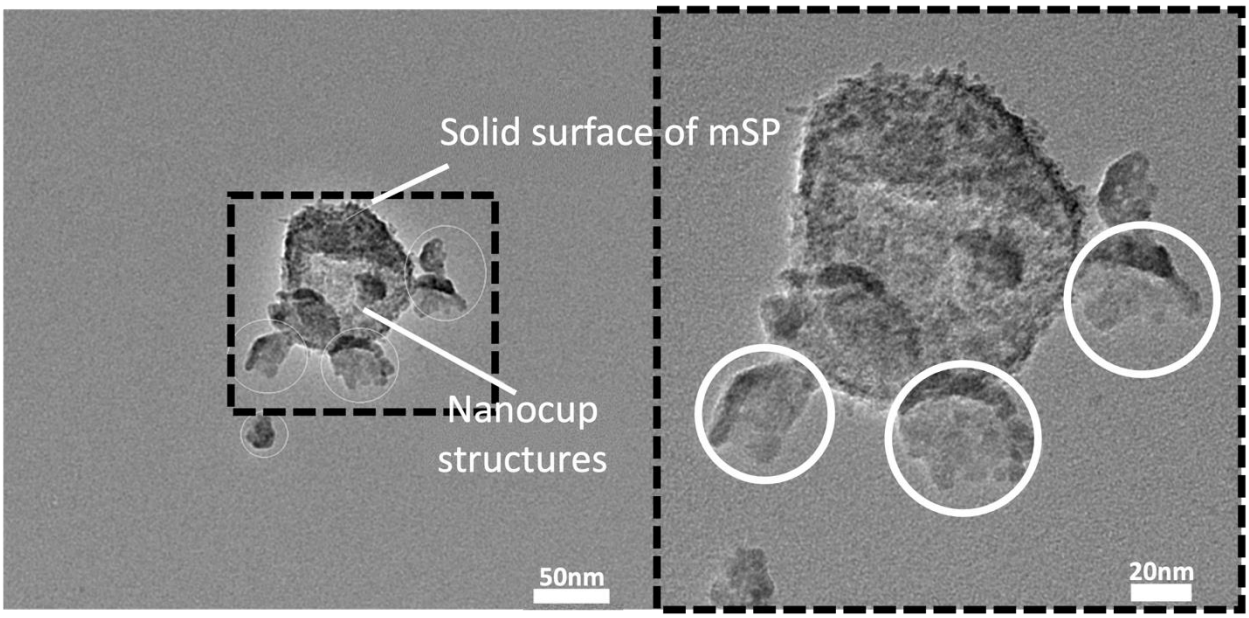

Figure S4 TEM images of broken mSP pieces at 30min reveals similar nanocups structures.

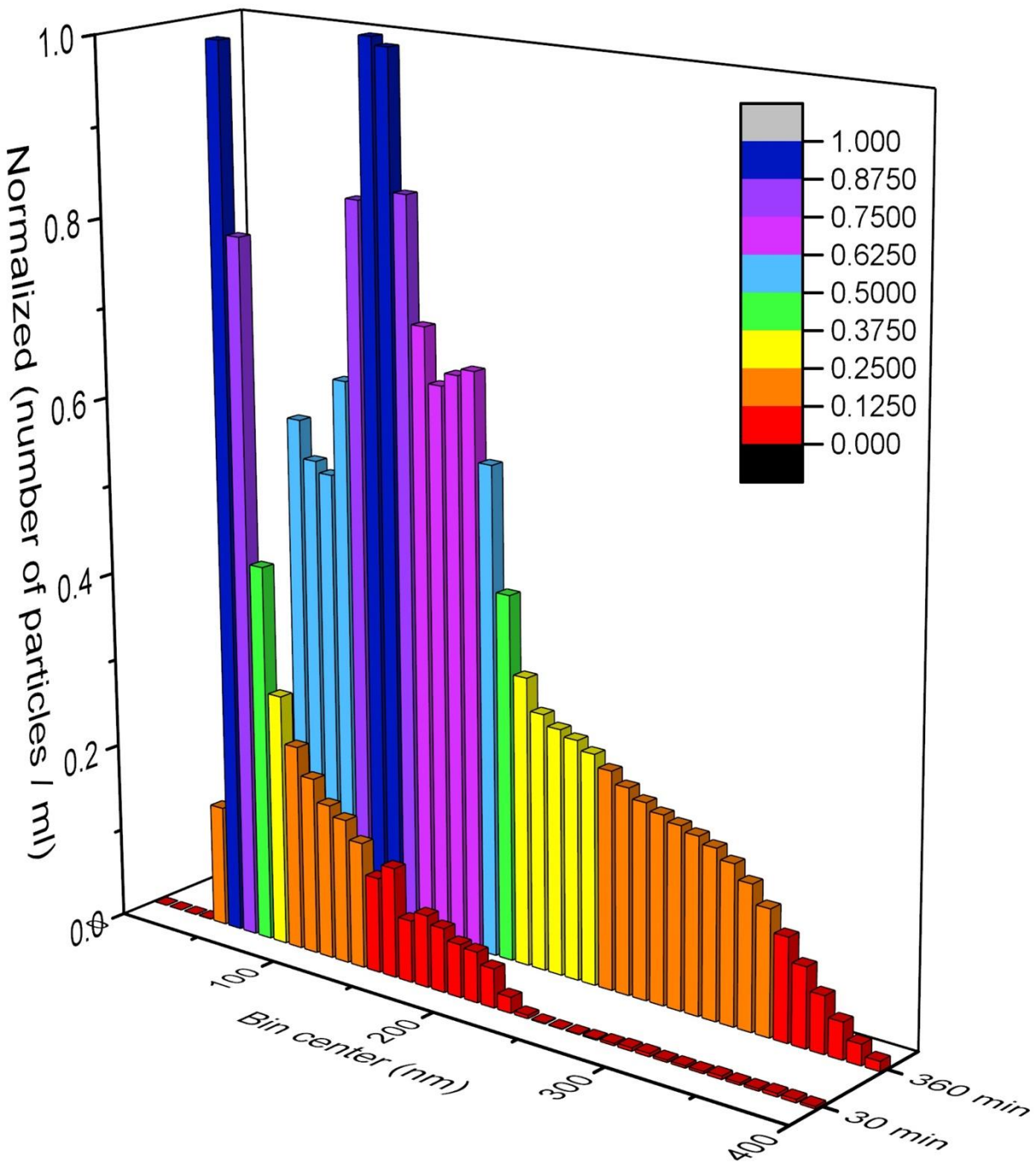

Figure S5 : Nanoparticle tracking analysis of mSP at 30 min and 360 min. As the optimum time (30min) passes, mSPs tends to aggregate.

1.2 mSPs with different amino acids

Different handed or derivative of cysteine such that *L*-cysteine, *D*-cysteine, and N-acetyl cysteine (NAC) are used to synthesize mSPs. Nevertheless, the type of stabilizer did not change the mSPs formation and their structures (**Figure S6**). However, for NAC mostly nanocup structures are observed at 30min (**Figure S6c**) Since the solubility of NAC is different than cysteine, it takes a longer time to complete the reaction and assembly of mSPs.

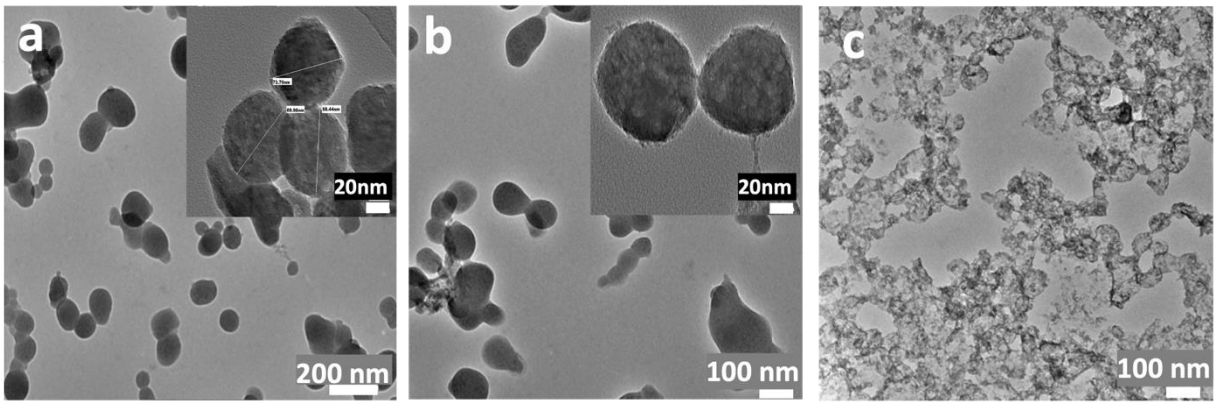

Figure S6 Same reaction condition with different stabilizer. (a) L-cysteine, (b) D-cysteine and (c) N-acetyl cysteine.

1.3 Statistical analysis of mSP and compartment volume

For the statistical analysis of the compartments, SEM-FIB ion milling (slice and view) was utilized since STEM tomography is not quite feasible for a cluster imaging and requires excess tomography data. SEM-FIB uses only the sliced particle images instead of tilted imaging; it is quite useful for analysis of multiple particles at once. We, therefore, chose an area that has a cluster with polydisperse mSPs for further investigation. Polydispersity is crucial to represent the entire mSP population (**Figure S7**). Seventeen mSPs in this cluster are first grouped based on location in the cluster and color-coded. Number of mSPs, each mSP size in diameter, average volume, and surface area of each color-coded area (blue, green, red, yellow, gray, and light blue) are measured (**Table S2).** We used **Figure S8** for calculation of the volume. As mSPs are not perfect spheres, volume measurements ($1.01*10^6 \pm 0.832 *10^6$ nm^3) are different than the calculation based on the average radius of a sphere with D=72.4 nm ($1.99 \pm 0.0853*10^5$ nm^3) **(Table S3)**.

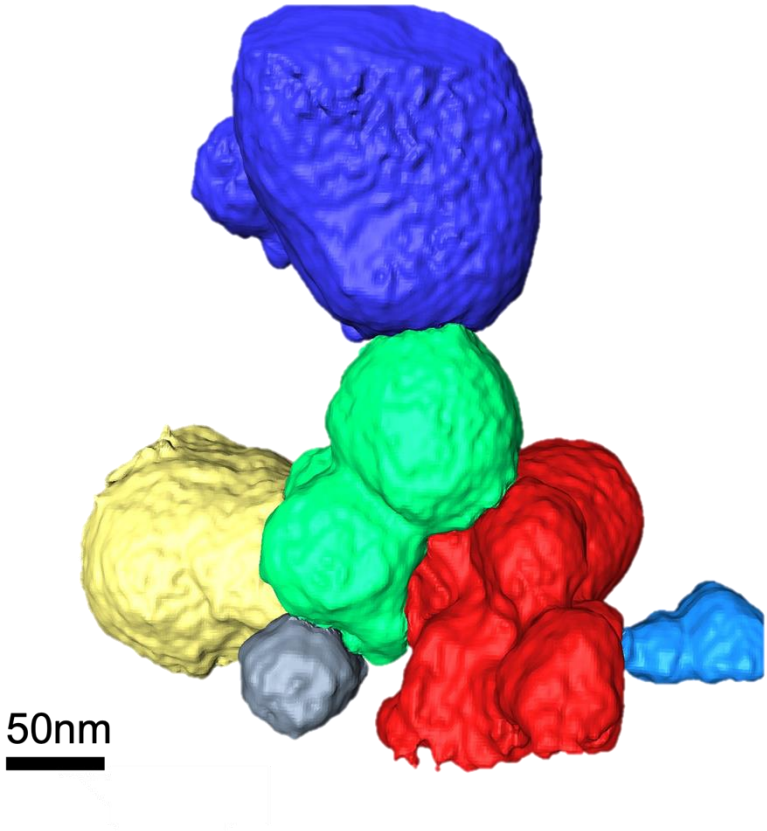

Figure S7 3D reconstruction images of mSPs acquired by SEM-FIB slice and view.

Table S2 Summary of volume and surface area of mSPs in Figure S7 based on 3D reconstruction analysis

Color area of mSPs	Number of mSP in each color area	Diameter of each mSP in each color (nm)	Total Volume (10^6 nm^3)	Total Surface Area (10^5 nm^2)
Blue	3	174.61, 74.98, 58.21	2.29	1.03
Green	5	95.84, 71.35, 47.58, 58.63, 53.26	1.12	0.69
Red	5	138.24, 68.07, 40.74, 68.97, 97.52	1.3	0.83
Yellow	1	124.29	1.15	0.67
Gray	1	60.29	0.10	0.12
Light Blue	2	57.5, 36.74	0.72	0.10

Table S3 Measured average diameter and volume of mSPs and compartments in Avizo

	Diameter (nm)	Volume (*10^6 nm^3)	Calculated volume (*10^5 nm^3) (D=72.4nm)
Supraparticle	78.05± 37.22	1.01 ± 0.0832	1.99 ± 0.0853
Compartment	5.2± 1.9	0.15± 0.048	* Volume is calculated based on average sized mSP from image J.
17 ± 5 % of the volume of supraparticles is compartments **37%**			

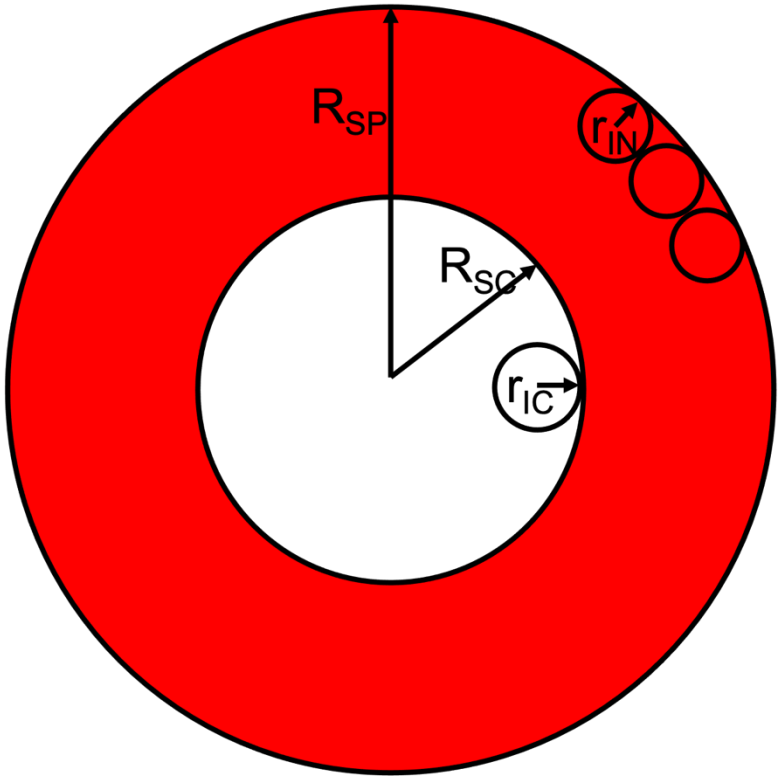

Figure S8 Geometrical model for number of NP, form chains, calculation in a mSP. mSP with radius R_{mSP}, NP with radius r_{IN}, compartments of mSP with radius R_{SC}, individual compartments with radius r_{IC}.

1.4 Surface Composition of mSPs

We performed X-ray photoelectron spectroscopy (XPS), and Fourier transform infrared spectroscopy (FTIR) analyses to investigate surface composition (**Figure S9 a-b**). High-resolution XPS data **(Figure S10)** suggests that cysteine binds to iron from the thiol group with the presence of Fe-S bond on FeS_2 surface and O-Fe-S bond on the Fe_2O_3 surface. S_{2p} spectra were fitted with several doublets corresponding to the $S_{2p\ 3/2\ -\ 1/2}$ components with a 1.2 eV spin-orbit splitting and area ratio of 0.5.[1] The S_{2p} binding energy at 162.30 eV and 163.50 eV should be assigned to FeS_2 $S2p_{3/2}$ and $S2p_{1/2}$ respectively. On the other hand, the S_{2p} binding energy at 167.20 eV and 168.40 eV should be assigned the sulfur from cysteine binds to Fe_2O_3 (S-Fe-O) $S2p_{3/2}$ and $S2p_{1/2}$ respectively. The peak at 167.20eV (5 eV shift of typical S-H peak 162.20eV) is indicating the chemisorption of cysteine via a sulfur group on Fe_2O_3 [2,3] (**Figure S10 a**). Fe_{2p} spectra of high-spin compounds exhibit multiple complex splitting and have satellite features. Therefore, five peaks are observed under Fe_{2p}. Two peaks for Fe_2O_3 $2p_{3/2}$ and $2p_{1/2}$, and two peaks for their satellite peaks. The fifth peak is $2p_{3/2}$ for FeS_2. Fe_{2p} in FeS_2 has low spin compounds; therefore, no split or satellite features observed (**Figure S10 b**). O_{1s} binding energy at 529.80 eV should be assigned to Fe_2O_3, and 531.5 eV should be assigned to O-C=O from L-cysteine (**Figure S10 c**). The cysteine binding on the NP confirmed with FT-IR (**Figure S9 a**). Amino acids generally show IR spectra specific to both carboxylate and primary amine salts since they exist as zwitterions.[4] Therefore, *L*-cysteine showed very broad peak for NH_3^+ stretch ($\nu(NH_3^+)$) at 3000-3500 cm^{-1} and COO^- stretch ($\nu(COO^-)$) at 1350-1700 cm^{-1} all are very typical amino acid IR spectra.[5] The weak S–H bend at 2550 cm^{-1} specifies a cysteine molecule (**Figure S9 a**). Asymmetric COO- and NH_3^+ stretching can cause a shift in the position in the IR spectra due to dipole moment change as when cysteine binds on the metal surface with high electron density. Weak S-H peak disappears in mSPs' IR spectra, and this verifies the covalent interaction of sulfur and iron (**Figure S9 a**). Therefore, cysteine binding to iron from the thiol group is confirmed, and the positive charge is explained by the NH_3^+ groups of the surface ligand (**Fig. 3j and Figure S*2*)**

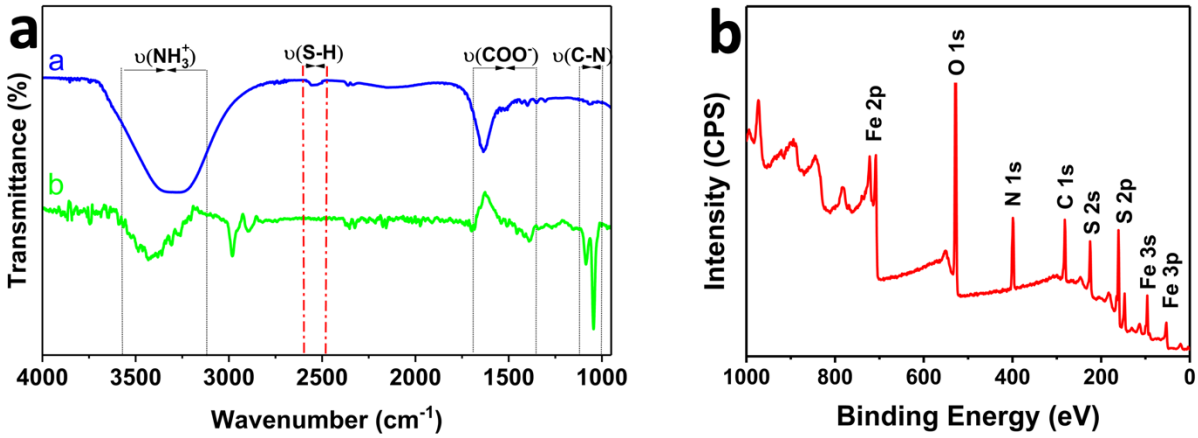

Figure S9 (a) FT-IR spectra of L-cysteine (a-blue) and mSP (b-green). (b) XPS survey spectrum of mSPs.

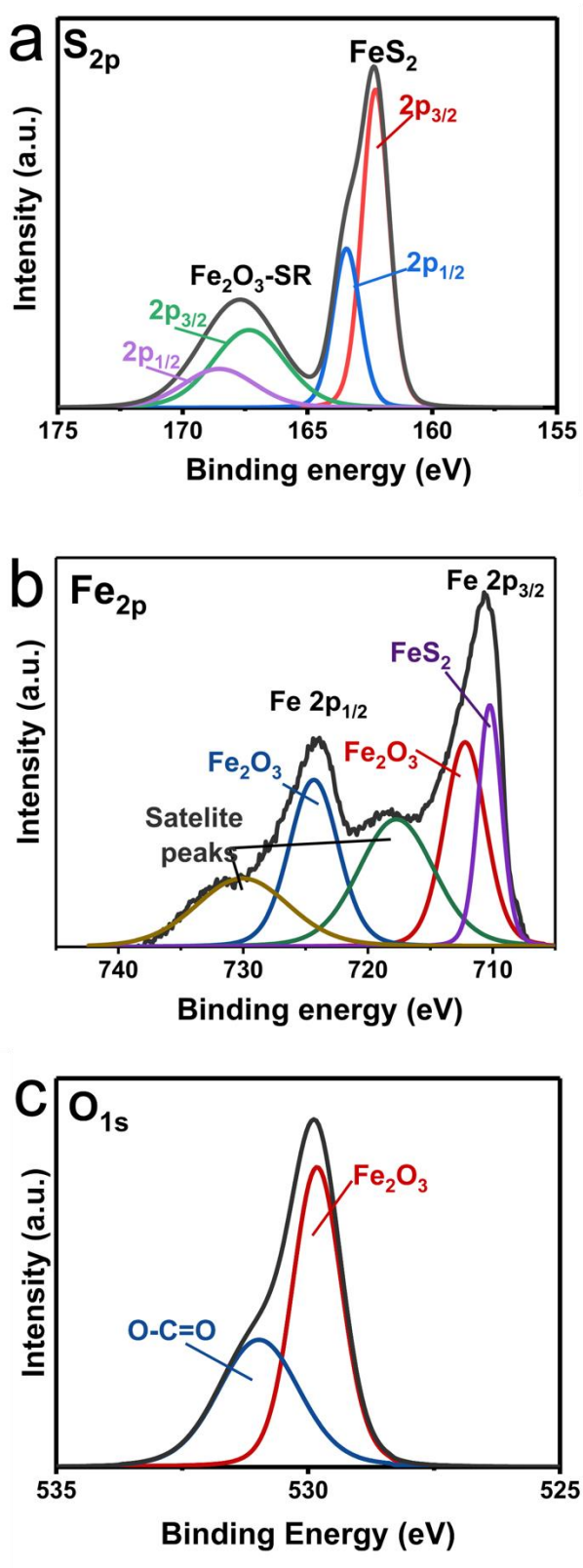

Figure S10 High resolution XPS spectra of (a) S_{2p} (b) Fe_{2p} and (c) O_{1s} of mSPs.

1.5 Photoluminescence analysis of mSP

We performed emission scanning and the stable emission peaks are seen between 320 nm - 650 nm which confirms the autofluorescence of mSPs (**Figure S11a**). We also performed lambda scanning under Leica SP8 confocal microscope to find the best excitation and corresponding emission wavelengths for future confocal imaging. Fluorescence intensity data from lambda scanning is entirely consistent with our fluorescence data and stays in the highest excitation range **(Figure S11f).** This data also shows the highest emission can be obtained when mSP suspension excited at 475nm and 500nm under confocal microscopy. Further imaging is continued with 475nm and 500 nm excitation with a 520-570 nm emission window. The resolution of the light microscopy is not enough to observe individual mSP; however, around 200nm aggregations of mSPs can be easily seen (**Figure S11 b-e**).

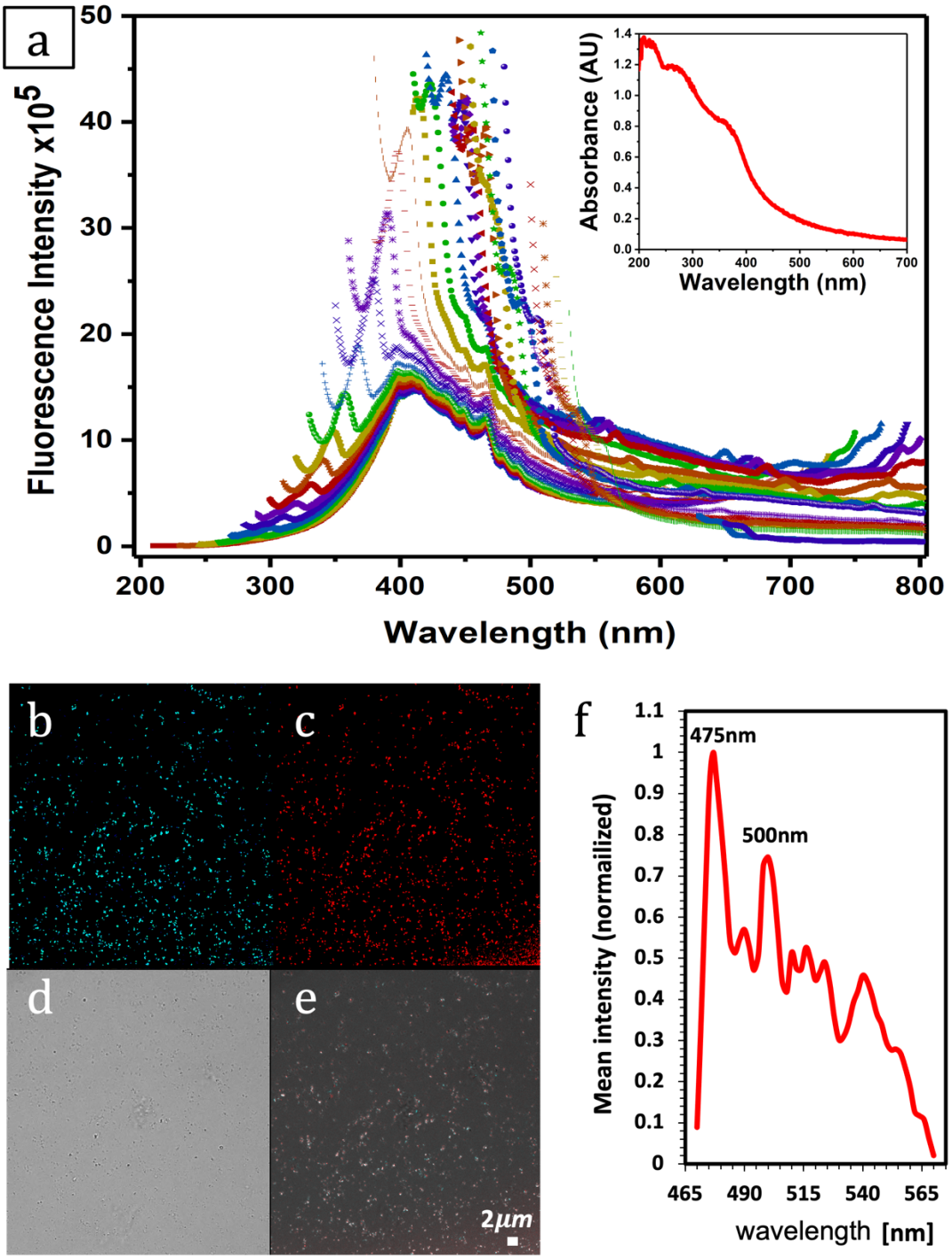

Figure S11 (a) Fluorescence emission of the mSP. The graph shows mSP emission at the excitation wavelengths from 200 to 600 every 10 nm increments. The graph in the insert shows UV-Vis absorbance spectrum of the mSP. (b-e) mSP suspension under confocal microscopy. (b) is excited at 475 nm and (c) is excited at 500 nm emission for both emission is 520-570nm. (d) DIC

image (e) overlay image. (f) Excitation spectrum in confocal microscopy shows 475nm and 500nm gives the highest emission intensity.

1.6 Chemical composition of Nanocups

To understand the mechanism of cup-like structure formation, we checked the composition of the nanocups. The nanocups are also composed of Fe, S, and O (**Figure S12**); the amount of Fe_2O_3 NPs is higher than FeS_2 NPs (**Table S4**). However, the amount of FeS_2 NP is higher in mSPs. Not packed FeS_2 NPs must be washed through washing steps while we collect the nanocups from the reaction. Color change during the reaction shows that NPs are self-assembled into first nanocups (15min) and then mSPs (30 min) with the effect of oxidation.

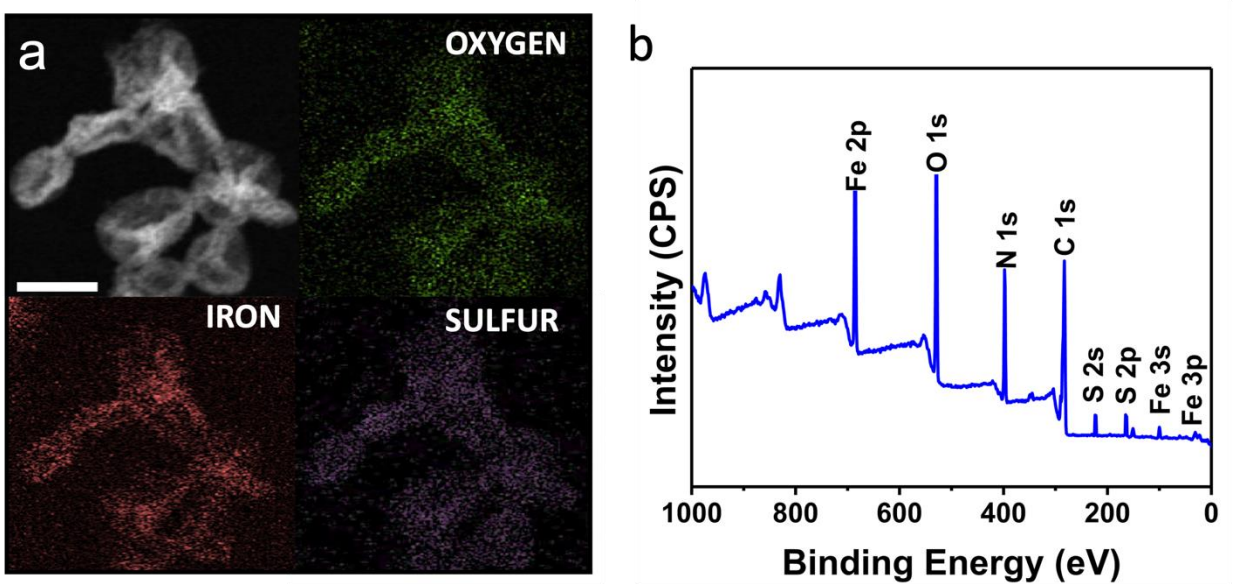

Figure S12 (a) Elemental analysis of the mSPs and location of iron, sulfur and oxygen elements in nanocups, (b) XPS survey spectrum of nanocups. Scale bar: (a)50nm

Table S4 Atomic percentage of elements nanocup intermediate obtained by EDS

Element	Atomic Percentage, %
Fe	42.8
S	13
O	44.2

1.7 Graph Theory

Graph theory (GT) in this study is a method that developed in our group[6] to graphically represent of assembled structures based on discretized nanoscale components and we calculate the complexity based on Randic *et al*.[7] In this study, the smallest component of the self-assembled structures, nanocups and mSPs, is disc like nanoparticles; and is represented as a K3 graph, which represent a 2-D structure (**Figure S13a**). We calculated complexity index (*CI*) of each structure based on augmented valence of an individual node. Same colored nodes are symmetrically equivalate and calculated once for *CI* calculations since repetitive motifs do not increase information content of the graph. Nonetheless all symmetrically equivalent classes of nodes are included in the summation process of the leading node if they are the in the nearest-neighbors group. For *CI* calculations we used **Equation S1** in where *k* is the number of edges stemming from the node, and *d* is the distance to the node.

Equation S1: Complexity index equation $$\sum_{d=0}^{\infty} \frac{\sum_{i=1}^{\infty} k_{i_d}}{2^d}$$

Based on **Equation S*1*** and K graphs[6] (**Figure S*13*a)** we calculated *CI* for the constituent NP as 4, for the nanocups as 18.75, for compartments as 8 and mSP as 19.5 (**Figure S13**). We also calculated CI for adenovirus as 25.125 (**Figure S14**).

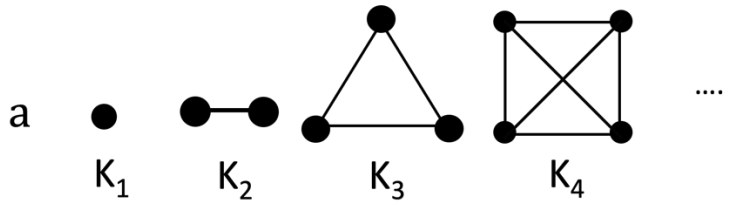

b

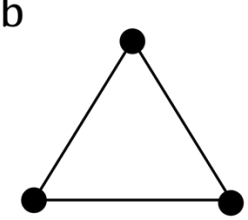

$$CI_{NP} = \frac{2}{2^0} + \frac{2+2}{2^1} = 4$$

c

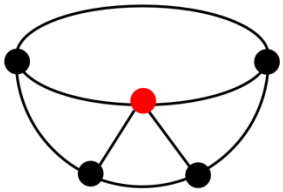

$$CI_{nanocups} = \left(\frac{4}{2^0} + \frac{4\times3}{2^1}\right) + \left(\frac{3}{2^0} + \frac{4+3+3}{2^1} + \frac{3}{2^2}\right) = 18.75$$

d

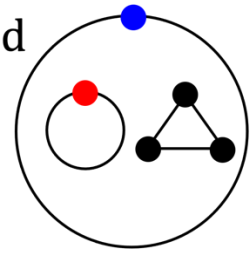

$$CI_{compartments} = \left(\frac{2}{2^0} + \frac{2+2}{2^1}\right) + \left(\frac{2}{2^0}\right) + \left(\frac{2}{2^0}\right) = 8$$

e

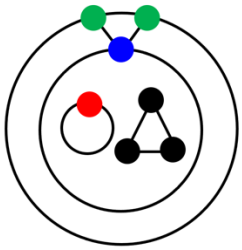

$$CI_{mSPs} = \left(\frac{2}{2^0} + \frac{2+2}{2^1}\right) + \left(\frac{2}{2^0}\right) + \left(\frac{4}{2^0} + \frac{2\times3}{2^1}\right) + \left(\frac{3}{2^0} + \frac{4+3}{2^1}\right) = 19.5$$

Figure S13 Complexity index calculation of (a) K_1- K_4 graphs for calculation GT (b) constituent NP (c) nanocups (d) compartments and (e) mSPs. Each sphere represents a node, and each line represents an edge. Same colored nodes are equivalate and calculated once for CI calculations.

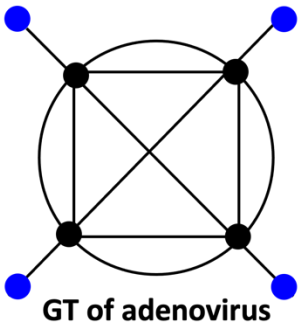

$$CI_{\text{adenovirus}} = \left(\frac{6}{2^0} + \frac{(3\times6)+(1\times1)}{2^1} + \frac{3\times1}{2^2}\right) + \left(\frac{1}{2^0} + \frac{1\times6}{2^1} + \frac{3\times6}{2^2} + \frac{3\times1}{2^3}\right) = 25.125$$

Figure S14 Complexity index calculation of crystal structure of human adenovirus.

1.8 mSP vs mSP-pDNA comparison

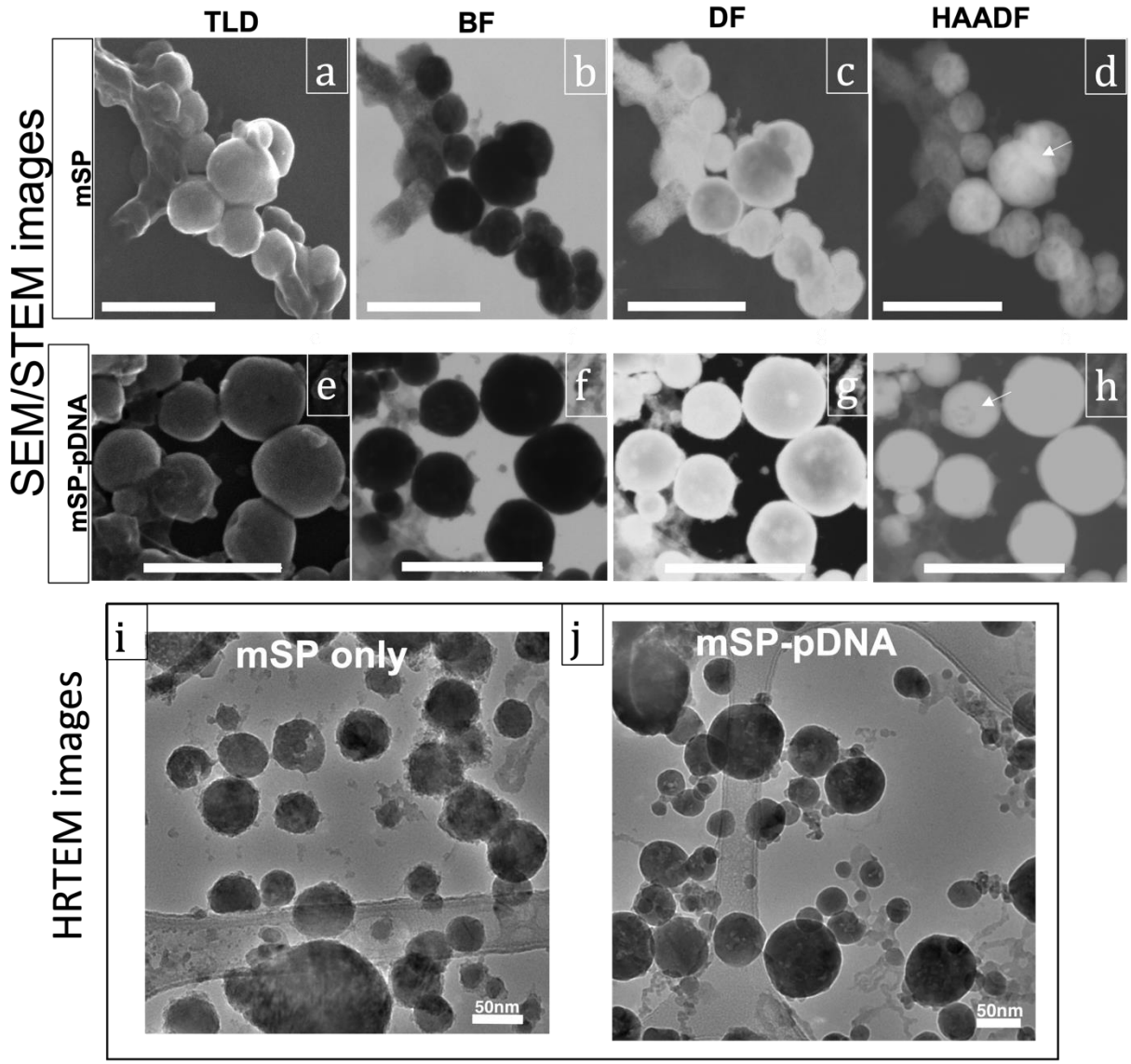

Figure S15 Comparison of mSP and mSP-DNA. STEM images of mSP (a-d) and mSP-pDNA (e-h) acquired with default Through the Lens Detector (TLD), Bright field (BF), Dark Field (DF) and High-angle annular dark field (HAADF) (STEM mode) detectors. HAADF shows compartments in mSP with darker color (pointed with arrow) in (d). In mSP-pDNA HAADF filled compartment. TEM images of mSP (i) and mSP-pDNA (j). Scale bar: (a-h) is 200nm, (i-J) is 50 nm.

1.9 Degradation assay of mSP-pDNA

mSP started to degrade at acidic conditions at pH 5.5 in water within 2hours (**Figure S16**) as seen in TEM images. TEM images show increasing NPs content as time progress after 30min (blue box), 1h (red box), and 2h (black box).

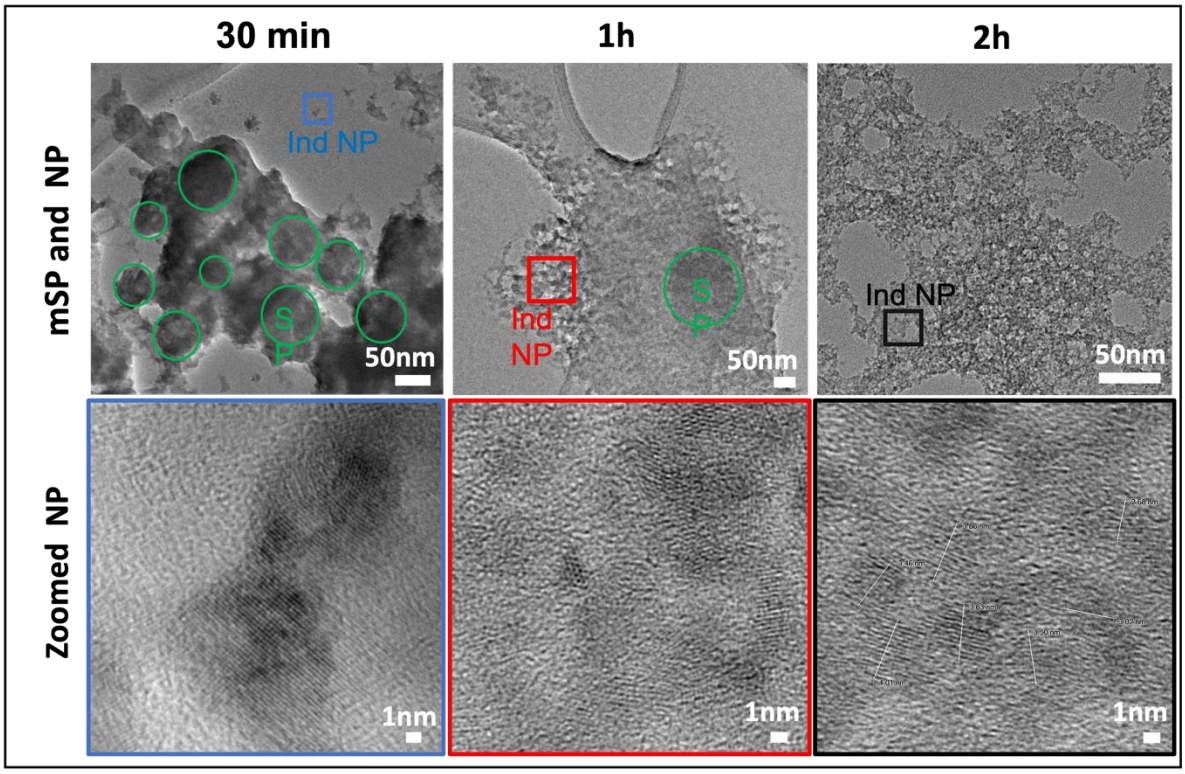

Figure S16 Degradation of mSP-pDNA under biologically relevant conditions. Each image zoomed on colored boxes for high resolution images. (Figure shows only samples in water pH 5.5).

1.10 mSP Concentration for Cytotoxicity

We calculated particle concentration before cellular experiments via nanoparticle tracking analysis (NTA) what gives the number of particles per ml. Particles are prepared in different concentration: 10^{11} particles/ml (1000x) and 10^{9} particles/ml (10x) (**Figure S17**). The cellular uptake is also a critical step for transfection. Hence, we performed cellular uptake before transfection to make time progress data of the uptake of mSPs. For this experiment, we used 10X concentration of mSP (~1000 mSPs per cell) and HEK293T cell, as this cell line is prominent for transfection experiments.

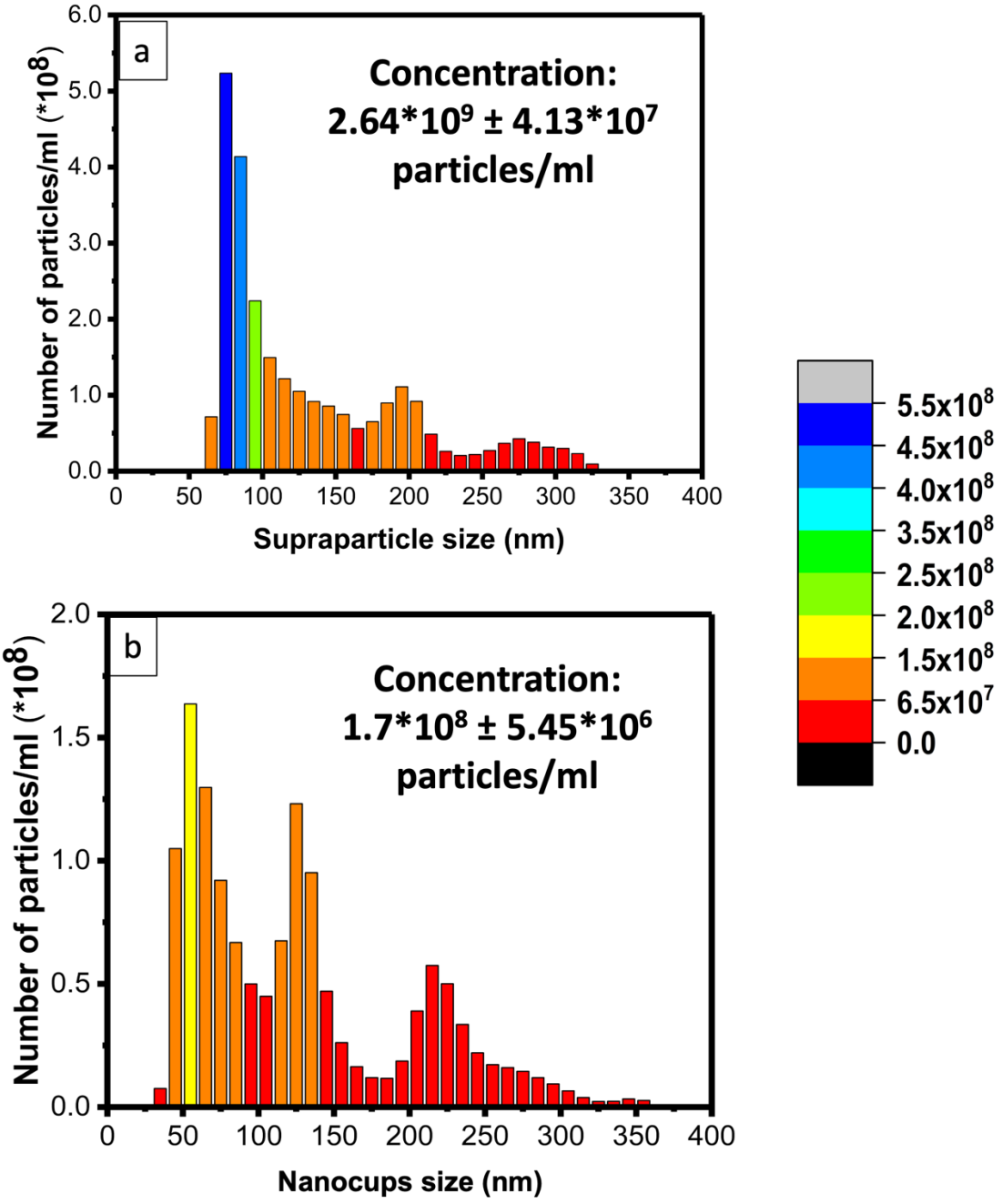

Figure S17 (a) NTA data for mSP at 30min (10x) and (b) nanocups at 15min (1x) concentration. The number of mSPs is important to calculate the amount of DNA and cytotoxicity. 10X mSPs gives 1000mSP per cells that is not toxic.

1.11 Cellular Uptake

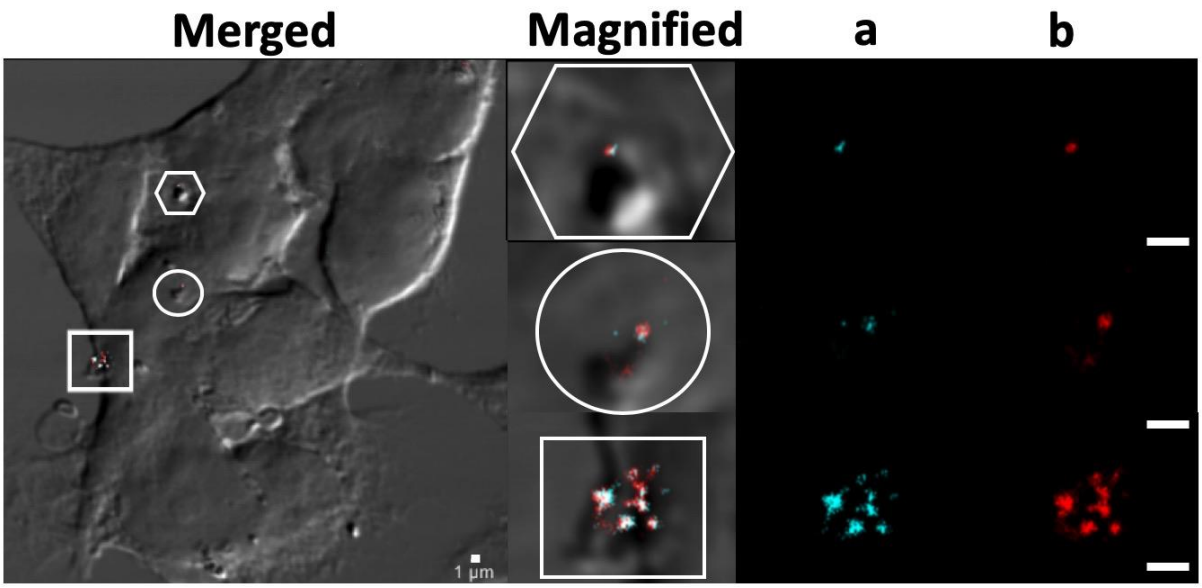

Figure S18 HEK cells treated with mSP for 1 hour. (a) is excited at 475 nm and (b) is excited at 500 nm. Emission for both excitations are 520-570nm. Scale bars: 1µm

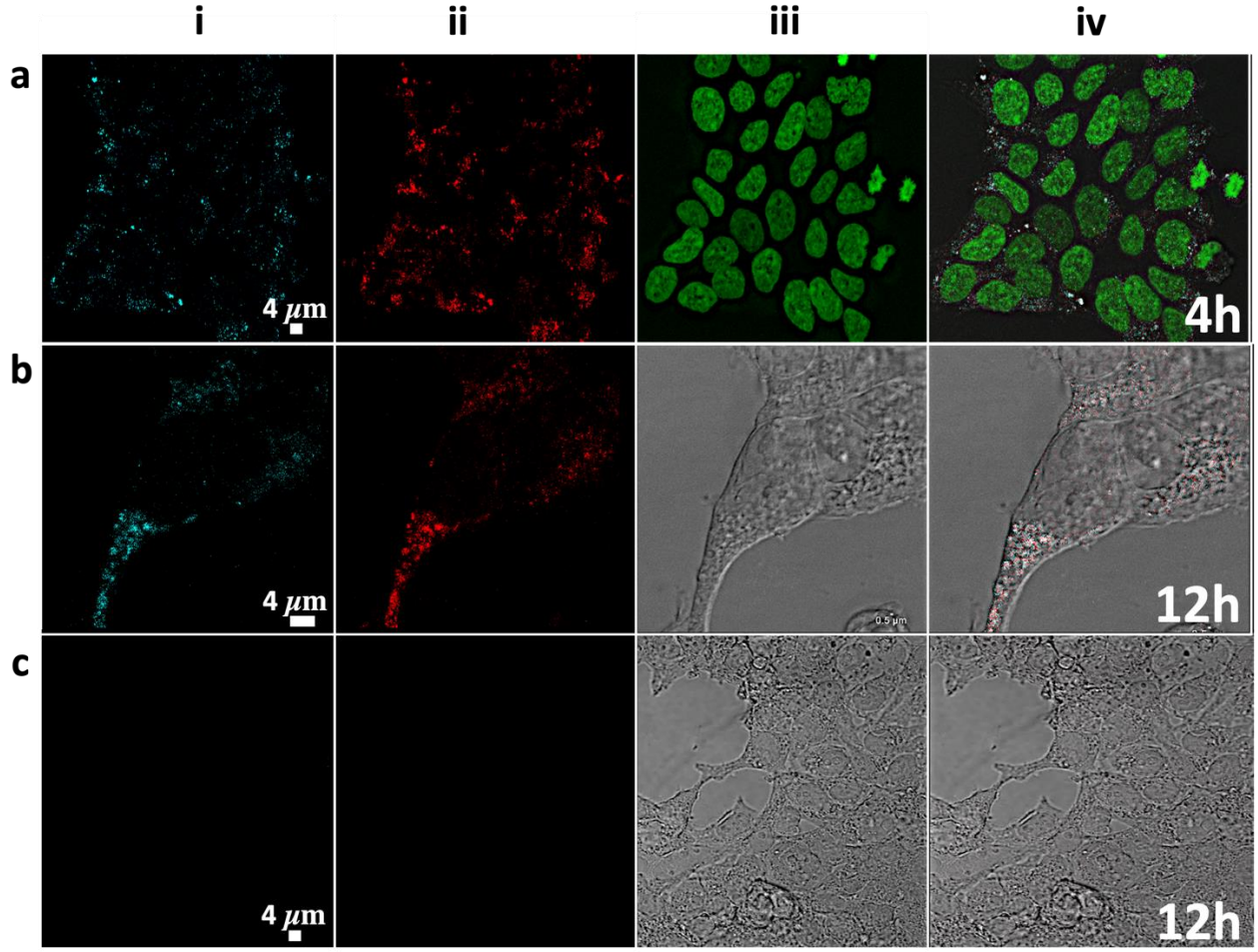

Figure S19 Cellular uptake confocal images. (a-b) HEK cells treated with mSPs. (c) HEK cells are not treated with mSP. (a) Cell treatment with mSP after 4h, (b-c) Cell treatment with mSP after 12h. All images are taken under same conditions, laser power, intensity and brightness are all same. (i) is excited at 475 nm and (ii) is excited at 500 nm; emission window for both excitations are 520-570 nm. (iii) DIC or DAPI images (iv) Merged image.

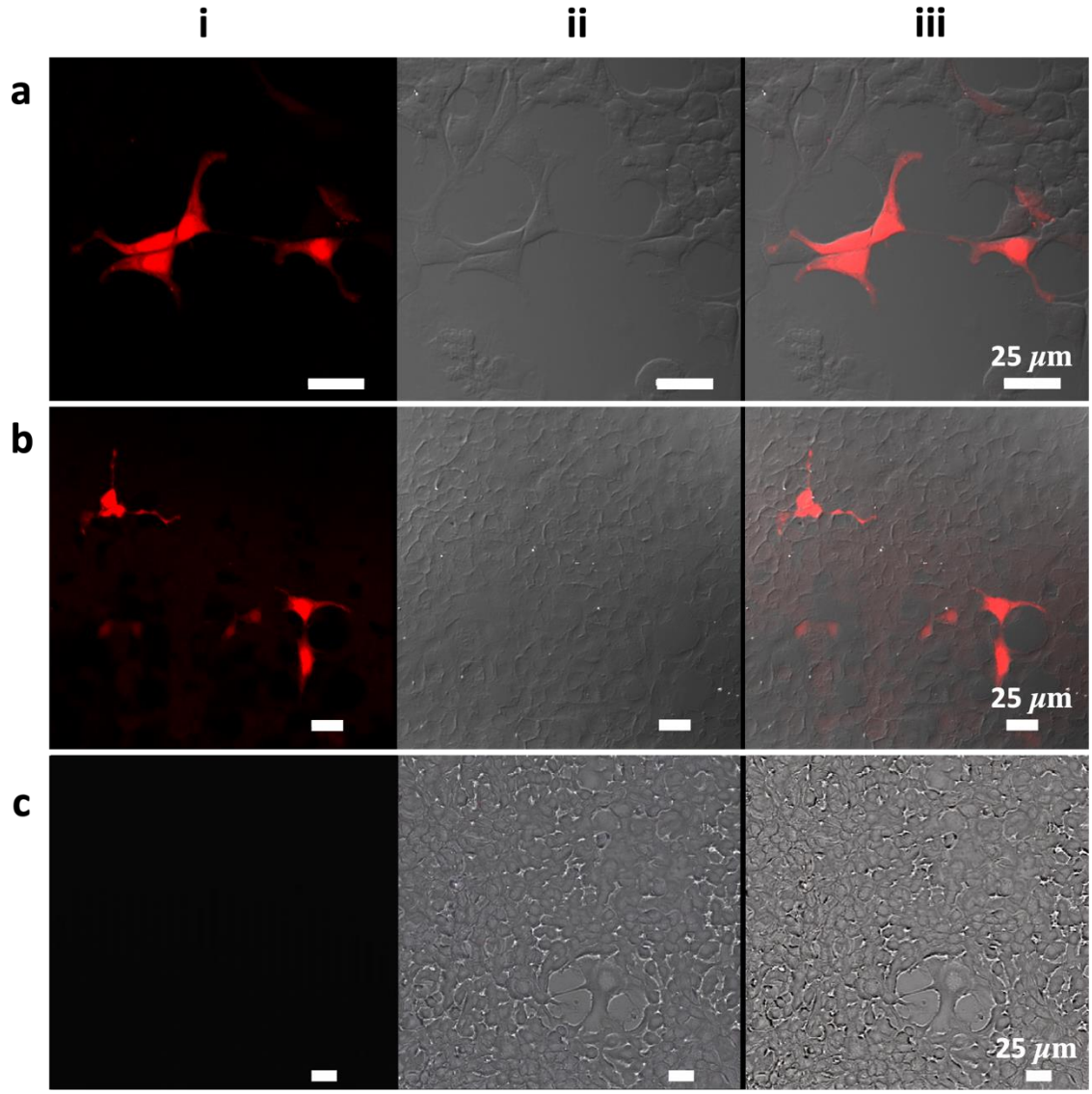

Figure S20 24h post-transfection comparison of mSP-pDNA and Lipofectamine. Supraparticle with DNA and lipofectamine. (a) mSP-pDNA (b) Lipofectamine (c) mSP only after 24h transfection. (i) Texas red filter (ii) DIC (iii) Merge image.

1.12 Thermal Stability

mSPs are dissolved in water and stored at room temperature (RT), in freezer (-20 °C) for >4 years to track the stability. mSP and mSP-pDNA are kept in oven (70 °C) for 50h to track thermal stability and protection of the DNA.

1.13 Comparison of viruses and mSP based on loading capacity

Adenovirus and mSP has similar loading capacity where adenovirus can be loaded up to 8kb[8] and mSP can be loaded >6kb.

Table S5: Comparison of adenovirus, lentivirus and mSP

	mSPs	Lentivirus	Adenovirus
Self-assembly	Inorganic NP (4-5nm)	Protein (4-5nm)	Protein (4-5nm)
Size	50-100nm	80-100nm	90-100nm
Loading capacity	>6kb	<8kb[8]	<8kb (Replication defective)[8]

1.14 Nanocup assembly

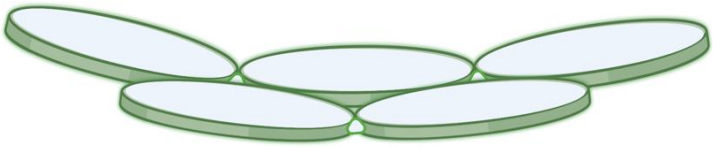

Figure S21: Self-assembly of anisotropic constituent platelet-like structures into nanocups. (Green color represents attractive forces, and white color represents repulsive forces)

REFERENCES

1. Alarcón, L. S., Cristina, L. J., Jia, J., Chen, L., Giglia, A., Pasquali, L., Sánchez, E. A., Esaulov, V. A. & Grizzi, O. Adsorption and thermal stability of 1,4 benzenedimethanethiol on InP(110). *Surf. Sci.* **664**, 101–109 (2017).

2. E. Mateo Marti, †, Ch. Methivier, and & Pradier*, C. M. (S)-Cysteine Chemisorption on Cu(110), from the Gas or Liquid Phase: An FT-RAIRS and XPS Study. (2004) doi:10.1021/LA048952W.

3. Ma, Z. & Han, H. One-step synthesis of cystine-coated gold nanoparticles in aqueous solution. *Colloids Surfaces A Physicochem. Eng. Asp.* **317**, 229–233 (2008).

4. Soomro, R. A., Nafady, A., Sirajuddin, Memon, N., Sherazi, T. H. & Kalwar, N. H. L-cysteine protected copper nanoparticles as colorimetric sensor for mercuric ions. *Talanta* **130**, 415–422 (2014).

5. Aryal, S., B.K.C., R., Dharmaraj, N., Bhattarai, N., Kim, C. H. & Kim, H. Y. Spectroscopic identification of SAu interaction in cysteine capped gold nanoparticles. *Spectrochim. Acta Part A Mol. Biomol. Spectrosc.* **63**, 160–163 (2006).

6. Jiang, W., Qu, Z. B., Kumar, P., Vecchio, D., Wang, Y., Ma, Y., Bahng, J. H., Bernardino, K., Gomes, W. R., Colombari, F. M., Lozada-Blanco, A., Veksler, M., Marino, E., Simon, A., Murray, C., Muniz, S. R., Moura, A. F. de, Kotov, N. A., de Moura, A. F., Kotov, N. A., Moura, A. F. de & Kotov, N. A. Emergence of complexity in hierarchically organized chiral particles. *Science (80-.).* **368**, 642–648 (2020).

7. Randić, M. & Plavšić, D. On the Concept of Molecular Complexity. *Croat. Chem. Acta* **75**, 107–116 (2002).

8. Ghosh, S., Brown, A. M., Jenkins, C. & Campbell, K. Viral Vector Systems for Gene Therapy: A Comprehensive Literature Review of Progress and Biosafety Challenges. *Appl. Biosaf.* **25**, 7–18 (2020).